Electronic Supplementary Material (ESI) for RSC Advances.

Identification of Preferentially Exposed Crystal Facets by X-ray Diffraction

Liping Zhang, Alexandre A. S. Gonçalves, and Mietek Jaroniec*

Department of Chemistry and Biochemistry, Kent State University, Kent, Ohio 44242, USA

Table S1. Selected examples of crystalline materials with preferentially exposed facets and their applications

Material	**Preferentially exposed facet(s)**	**Application**	**Ref.**
Ag_3PO_4 rhombic dodecahedron	{110}	Photocatalytic degradation of rhodamine B (RhB) and methyl orange (MO)	1
Ag_3PO_4 cube	{100}		
Bi_2MoO_6 nanosheets	{001}	Photocatalytic removal of NO	2
BiOBr nanosheets	{001}	Photocatalytic synthesis of NH_3 using N_2	3
BiOCl nanosheets	{001} or {010}	Photocatalytic degradation of MO	4
BiOCl nanosheets	{001}	Photocatalytic RhB degradation	5
$BiOIO_3$ nanoplates	{010} and {100}	Photocatalytic CO_2 reduction	6
$BiVO_4$ sheet	(040)	Photocatalytic H_2O oxidation	7
$BiVO_4$ nanoplates	(040)	Photocatalytic H_2O oxidation	8
$BiVO_4$ photoanode	(001)	Photoelectrochemical H_2O oxidation	9
$BiVO_4$ nanosheets	{010}	Photocatalytic H_2O oxidation	10
CeO_2 nanocubes	{100}	Oxygen storage	11
Co_3O_4 nanosheets	{112}	Catalytic oxidation of trace C_2H_4	12
Mesoporous Co_3O_4	{110}		
Co_3O_4 dodecahedra	{111}	Photocatalytic CO_2 reduction	13
Co_3O_4 cube	(001)	Anode material for Li-ion batteries	14
Co_3O_4 polyhedra	(001) and (111)		
Co_3O_4 octahedra	(111)		
Fe_2O_3 nanosheets	(110)	Lithium storage and photocatalytic H_2O oxidation	15
Fe_2PO_5 decahedra	{010} and {110}	Electrocatalytic H_2O oxidation	16
Fe_2PO_5 octahedra	{110}		
CoP	(211)	Electrocatalytic O_2 reduction in zinc-air batteries	17
Ni_3S_2 nanosheets	$\{\bar{2}10\}$	Electrocatalyst for overall H_2O splitting	18
Pt nanocubes	{100}	/	19
Pt nanotetrahedra	{111}		
Pt hollow nanocubes	{111}	Catalytic O_2 reduction in fuel cells	20
Pt nanoplates	(111)	Electrocatalytic O_2 reduction	21
TiO_2 polyhedra	{001}	Photocatalytic decomposition of methylene blue	22
TiO_2 nanosheets	(001)	Lithium storage for Li-ion batteries	23
TiO_2 (anatase) nanobelts	(101)	Photocatalytic degradation of MO	24
TiO_2 (anatase) decahedra	{001}	/	25
TiO_2 (anatase) decahedra	{101}	Photocatalytic reduction of fluorogenic molecules	26
TiO_2 (anatase) decahedra	{001} or {101}	Photocatalytic conversion of CH_3OH into H_2	27

References

1 Y. Bi, S. Ouyang, N. Umezawa, J. Cao and J. Ye, *J. Am. Chem. Soc.*, 2011, **133**, 6490-6492.

2 S. Wang, X. Ding, X. Zhang, H. Pang, X. Hai, G. Zhan, W. Zhou, H. Song, L. Zhang, H. Chen and J. Ye, *Adv. Funct. Mater.*, 2017, **27**, 1703923.

3 X. Xue, R. Chen, H. Chen, Y. Hu, Q. Ding, Z. Liu, L. Ma, G. Zhu, W. Zhang, Q. Yu, J. Liu, J. Ma and Z. Jin, *Nano Lett.*, 2018, **18**, 7372-7377.

4 J. Jiang, K. Zhao, X. Xiao and L. Zhang, *J. Am. Chem. Soc.*, 2012, **134**, 4473-4476.
5 M. Guan, C. Xiao, J. Zhang, S. Fan, R. An, Q. Cheng, J. Xie, M. Zhou, B. Ye and Y. Xie, *Journal of the American Chemical Society*, 2013, **135**, 10411-10417.
6 F. Chen, H. Huang, L. Ye, T. Zhang, Y. Zhang, X. Han and T. Ma, *Adv. Funct. Mater.*, 2018, **28**, 1804284.
7 D. Wang, H. Jiang, X. Zong, Q. Xu, Y. Ma, G. Li and C. Li, *Chem. Eur. J.*, 2011, **17**, 1275-1282.
8 G. Xi and J. Ye, *Chemical Communications*, 2010, **46**, 1893.
9 H. S. Han, S. Shin, D. H. Kim, I. J. Park, J. S. Kim, P.-S. Huang, J.-K. Lee, I. S. Cho and X. Zheng, *Energy Environ. Sci.*, 2018, **11**, 1299-1306.
10 C. Dong, S. Lu, S. Yao, R. Ge, Z. Wang, Z. Wang, P. An, Y. Liu, B. Yang and H. Zhang, *ACS Catal.*, 2018, **8**, 8649-8658.
11 X. Hao, A. Yoko, C. Chen, K. Inoue, M. Saito, G. Seong, S. Takami, T. Adschiri and Y. Ikuhara, *Small*, 2018, **14**, 1802915.
12 C. Y. Ma, Z. Mu, J. J. Li, Y. G. Jin, J. Cheng, G. Q. Lu, Z. P. Hao and S. Z. Qiao, *J. Am. Chem. Soc.*, 2010, **132**, 2608-2613.
13 L. Wang, J. Wan, Y. Zhao, N. Yang and D. Wang, *J. Am. Chem. Soc.*, 2019, **141**, 2238-2241.
14 X. Xiao, X. Liu, H. Zhao, D. Chen, F. Liu, J. Xiang, Z. Hu and Y. Li, *Adv. Mater.*, 2012, **24**, 5762-5766.
15 J. Zhu, Z. Yin, D. Yang, T. Sun, H. Yu, H. E. Hoster, H. H. Hng, H. Zhang and Q. Yan, *Energy Environ. Sci.*, 2013, **6**, 987-993.
16 Y. Wu, Y. Meng, J. Hou, S. Cao, Z. Gao, Z. Wu and L. Sun, *Adv. Funct. Mater.*, 2018, **28**, 1801397.
17 H. Li, Q. Li, P. Wen, T. B. Williams, S. Adhikari, C. Dun, C. Lu, D. Itanze, L. Jiang, D. L. Carroll, G. L. Donati, P. M. Lundin, Y. Qiu and S. M. Geyer, *Adv. Mater.*, 2018, **30**, 1705796.
18 L.-L. Feng, G. Yu, Y. Wu, G.-D. Li, H. Li, Y. Sun, T. Asefa, W. Chen and X. Zou, *J. Am. Chem. Soc.*, 2015, **137**, 14023-14026.
19 C.-Y. Chiu, Y. Li, L. Ruan, X. Ye, C. B. Murray and Y. Huang, *Nat. Chem.*, 2011, **3**, 393.
20 W. Wang, X. Li, T. He, Y. Liu and M. Jin, *Nano Lett.*, 2019, **19**, 1743-1748.
21 H. Liu, P. Zhong, K. Liu, L. Han, H. Zheng, Y. Yin and C. Gao, *Chem. Sci.*, 2018, **9**, 398-404.
22 S. Liu, J. Yu and M. Jaroniec, *J. Am. Chem. Soc.*, 2010, **132**, 11914-11916.
23 J. S. Chen, Y. L. Tan, C. M. Li, Y. L. Cheah, D. Luan, S. Madhavi, F. Y. C. Boey, L. A. Archer and X. W. Lou, *J. Am. Chem. Soc.*, 2010, **132**, 6124-6130.
24 N. Wu, J. Wang, D. N. Tafen, H. Wang, J.-G. Zheng, J. P. Lewis, X. Liu, S. S. Leonard and A. Manivannan, *J. Am. Chem. Soc.*, 2010, **132**, 6679-6685.
25 H. G. Yang, C. H. Sun, S. Z. Qiao, J. Zou, G. Liu, S. C. Smith, H. M. Cheng and G. Q. Lu, *Nature*, 2008, **453**, 638-641.
26 T. Tachikawa, S. Yamashita and T. Majima, *J. Am. Chem. Soc.*, 2011, **133**, 7197-7204.
27 T. R. Gordon, M. Cargnello, T. Paik, F. Mangolini, R. T. Weber, P. Fornasiero and C. B. Murray, *J. Am. Chem. Soc.*, 2012, **134**, 6751-6761.

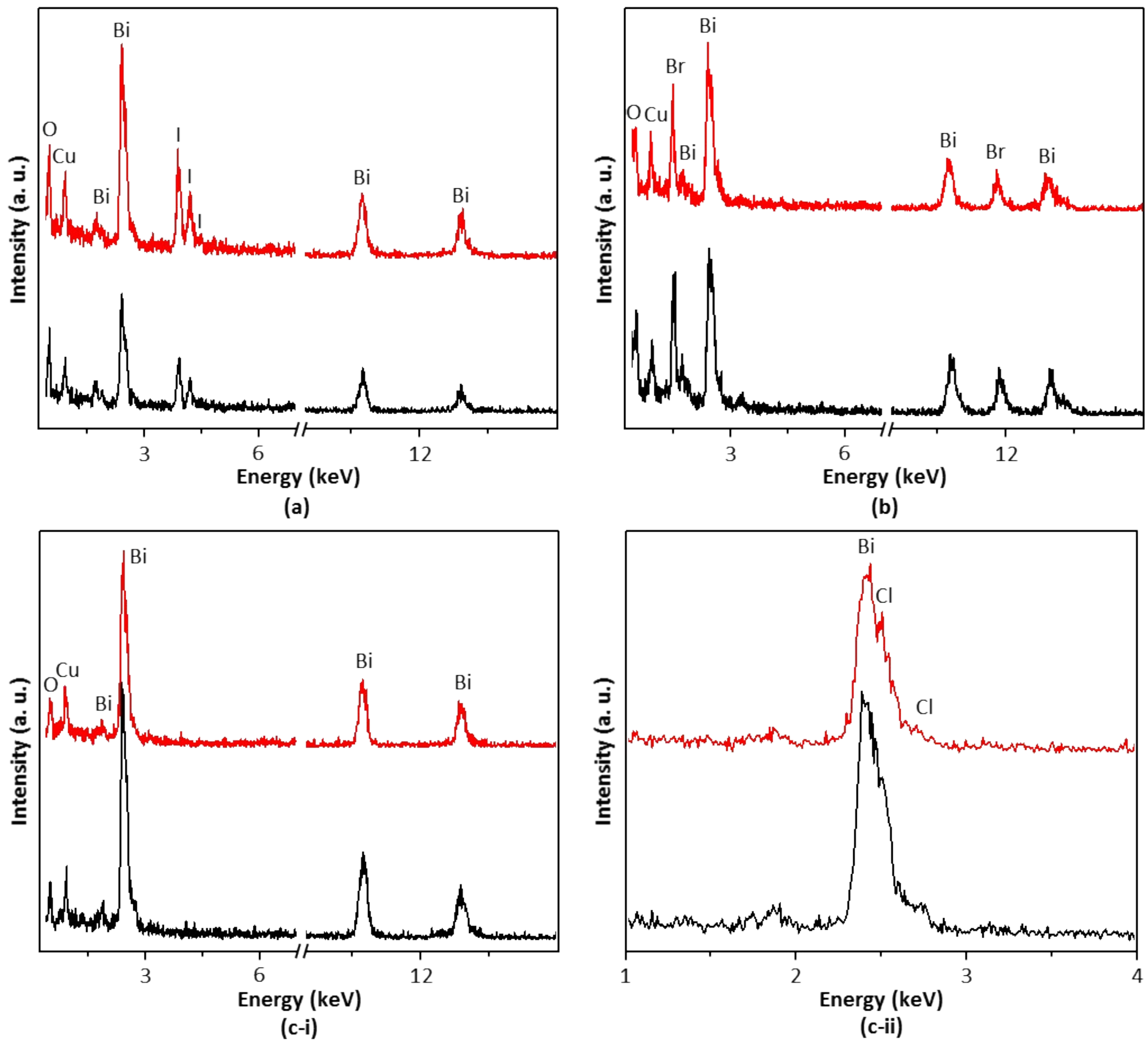

Fig. S1 EDX spectra recorded at two different areas of the synthesized (a) BiOI, (b) BiOBr, and (c) BiOCl samples. The peaks of Cu are attributable to the use of Cu grids.

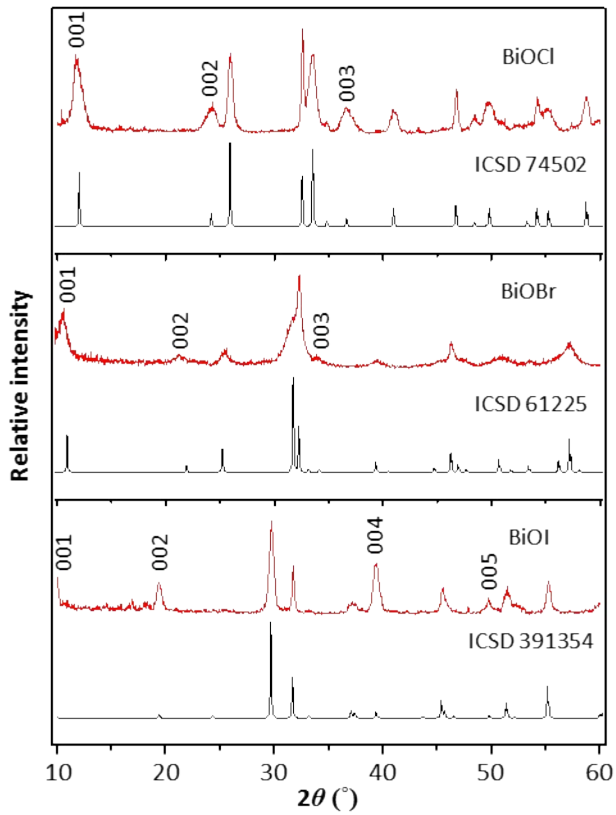

Fig. S2 XRD patterns of the synthesized BiOX samples.

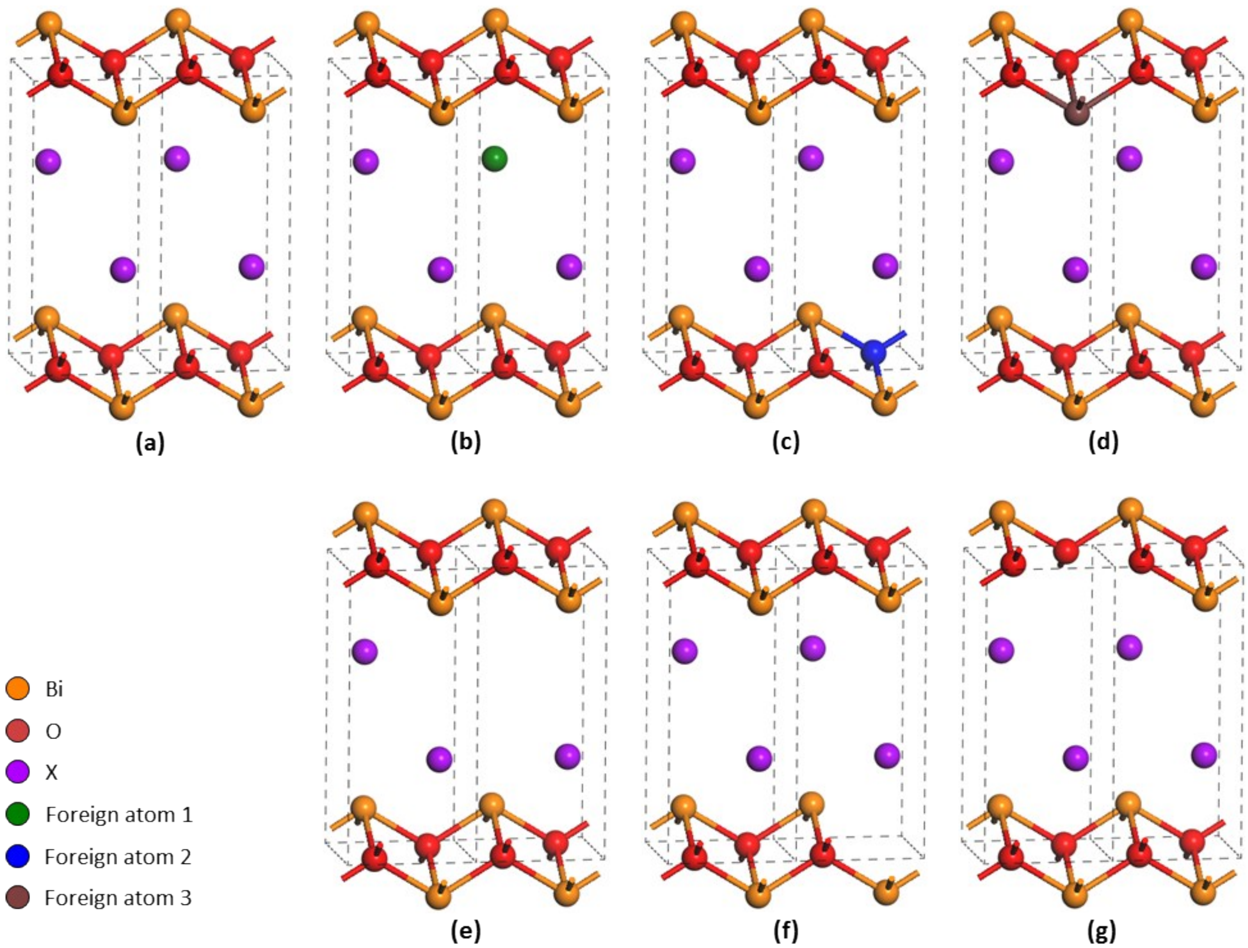

Fig. S3 Crystal structures of (a) BiOX, (b)-(d) BiOX doped with foreign ions, and (e-g) BiOX with vacancies.

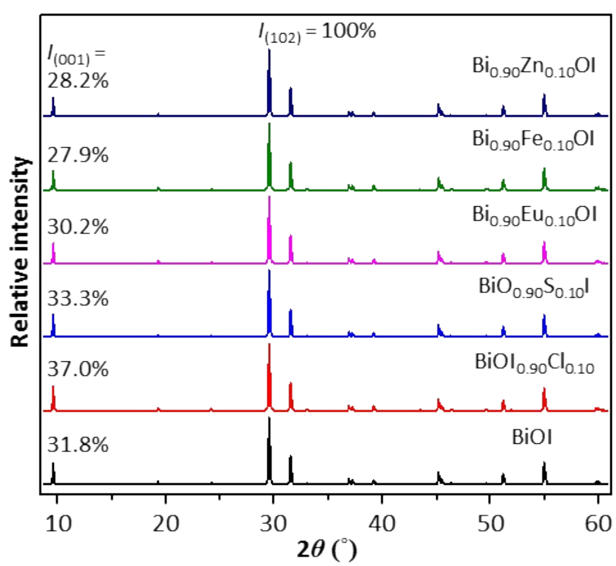

Fig. S4 Simulated XRD patterns of BiOI doped with various elements.

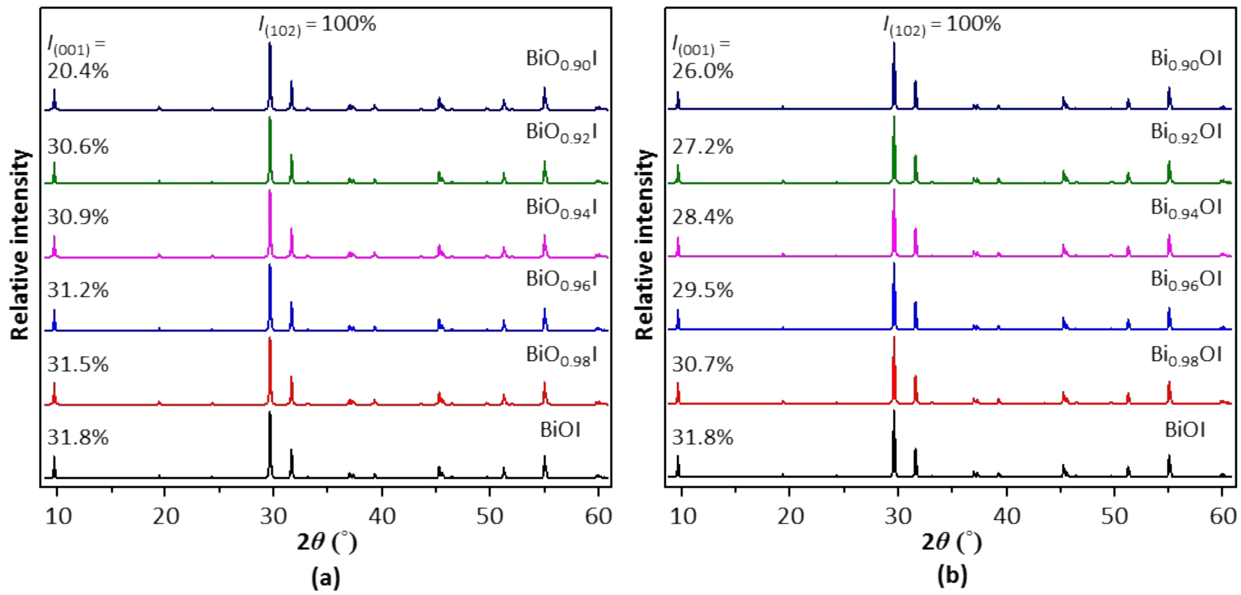

Fig. S5 Simulated XRD patterns of BiOI with various amounts of (a) O and (b) Bi vacancies.

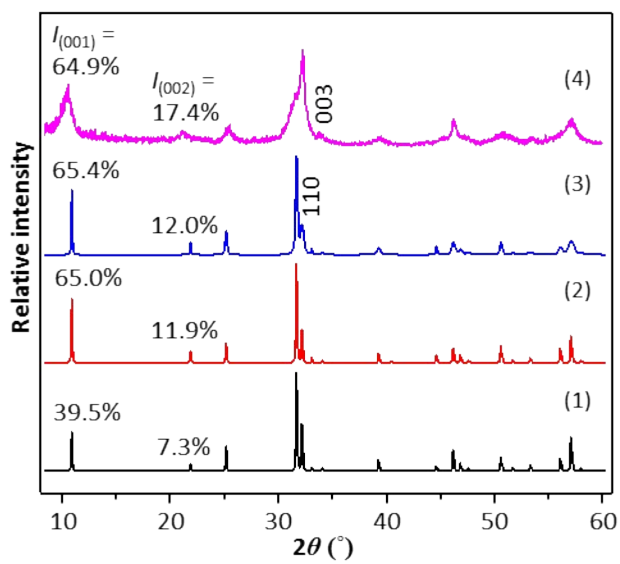

Fig. S6 Simulated (1-3) and experimental (4) XRD patterns of BiOBr. Pattern 1, bulk BiOBr without preferred orientation or anisotropic broadening; pattern 2, preferred orientation in [001] (March/Dollase parameter = 0.828); pattern 3, (110) broadening (anisotropic parameter = 1.5).

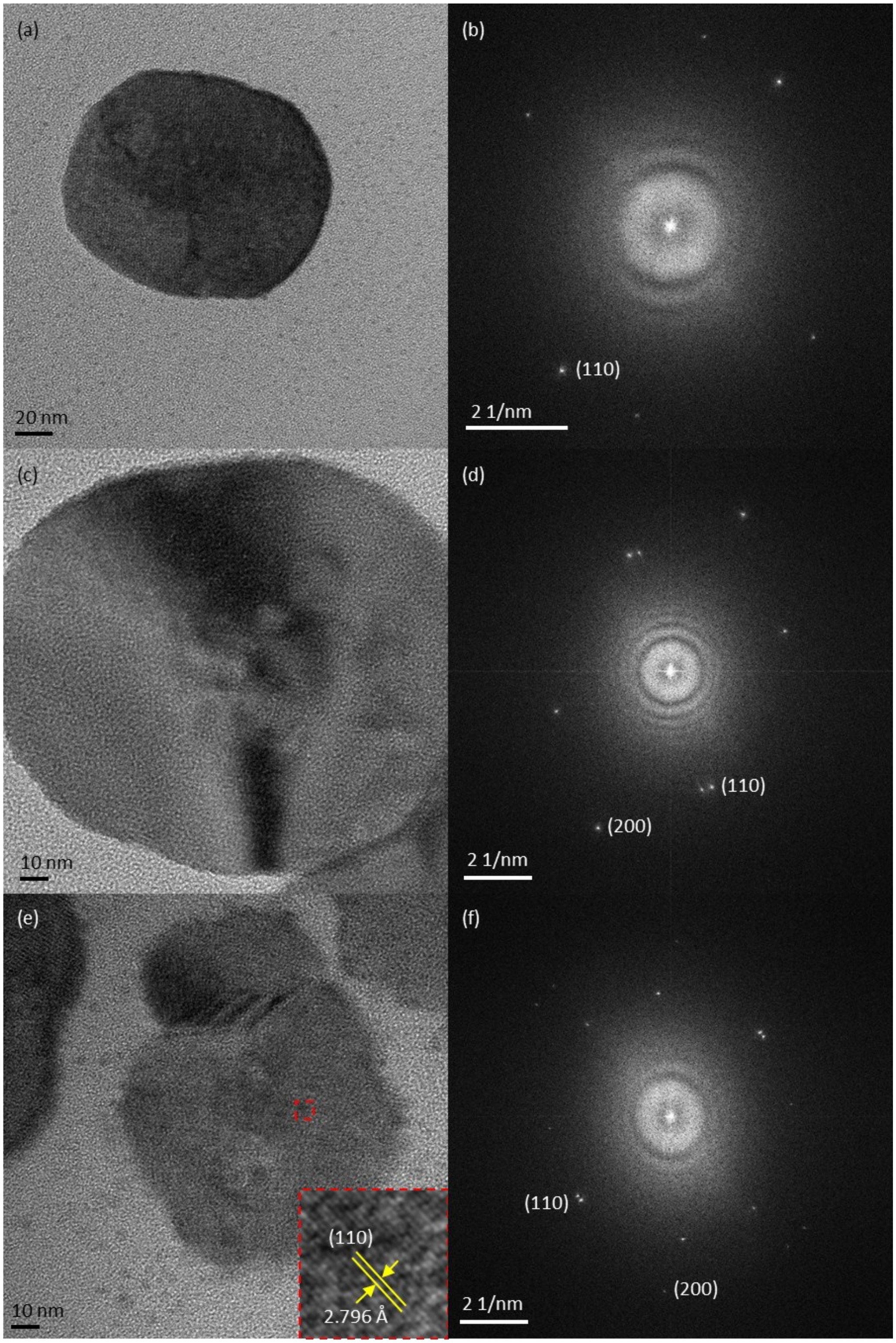

Fig. S7 (a, c, e) TEM images of BiOI nanoplates and (b, d, f) the corresponding fast Fourier transforms (FFTs). The insert of (e) is the magnified image of the red frame-enclosed area.

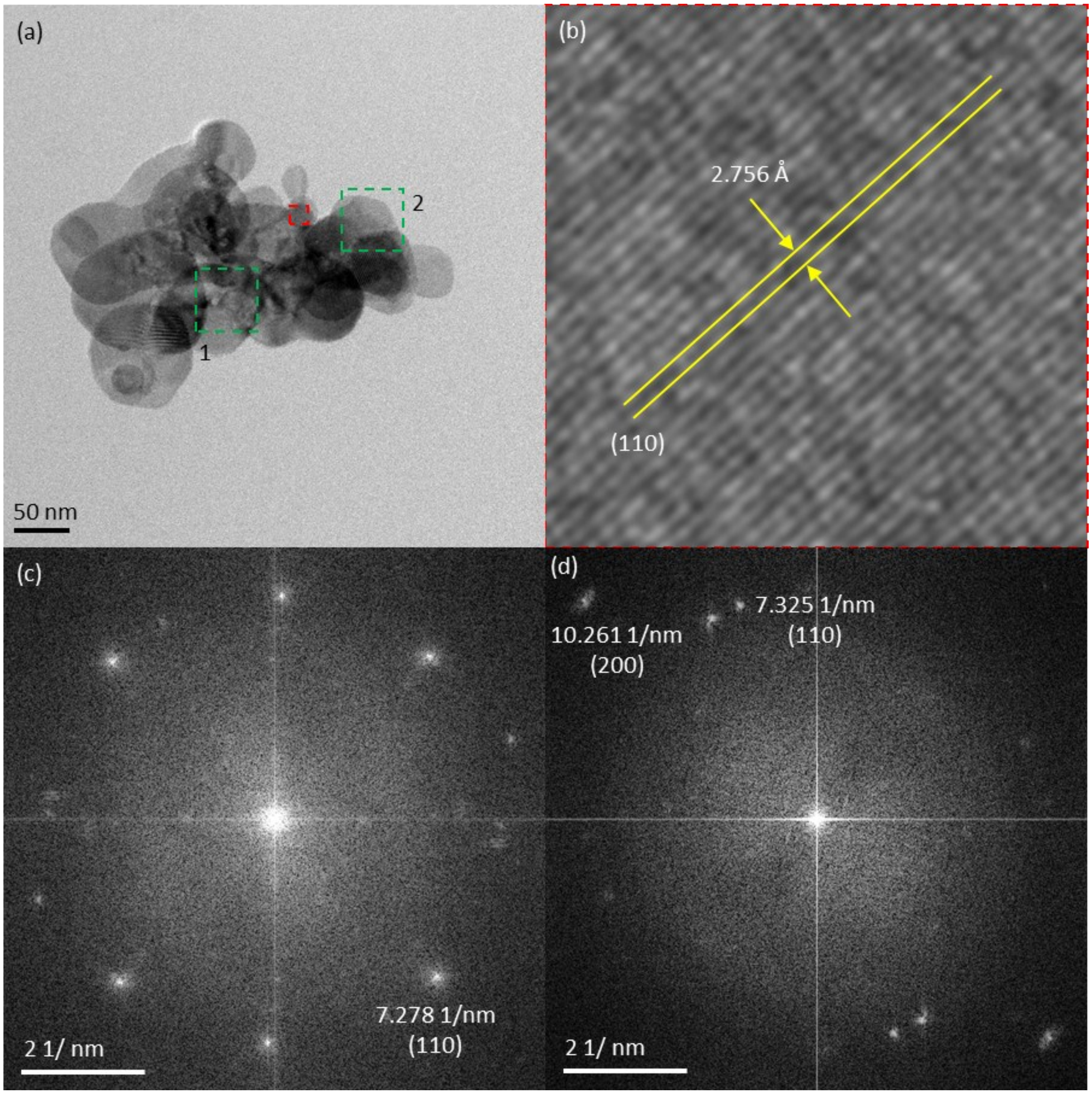

Fig. S8 (a) TEM image of BiOCl, (b) magnified image of the red frame-enclosed area, (c) and (d) FFTs of the green-colored frames 1 and 2, respectively, in (a).